VOLUME 32 NUMBER 2 April 2026
pISSN 2287-2728
eISSN 2387-285X

CLINICAL and MOLECULAR HEPATOLOGY

The forum for latest knowledge of hepatobiliary diseases

CV outcomes of oral antidiabetics in MASLD

Network meta-analysis of liver transplant criteria
ERBB3 blockade sensitizes HCC to regorafenib
ACSS2 as a metabolic target in HBV-related HCC

KASL

pISSN 2287-2728
eISSN 2287-285X

Clinical & Molecular Hepatology

https://doi.org/10.3350/cmh.2025.1252
Clinical and Molecular Hepatology 2026;32:843-865

Original Article

PRMT1-mediated asymmetric dimethylation of arginine residue 602 in DDX1 promotes cholangiocarcinoma progression

Wenzheng Liu*, Yangwei Liao*, Yiyang Kuai*, Xin Gao, Xingmin Yan, Jingjing Li, Junsheng Chen, Jukun Su, Jingcong Zhou, Yizhu Kong, Siqin Huang, Zhiwei Zhang, Feng Peng, Bing Wang, and Yongjun Chen

Division of Hepato-Pancreato-Biliary Surgery, Tongji Hospital, Tongji Medical College, Huazhong University of Science & Technology, Wuhan, Hubei, P.R.China

Graphical Abstract

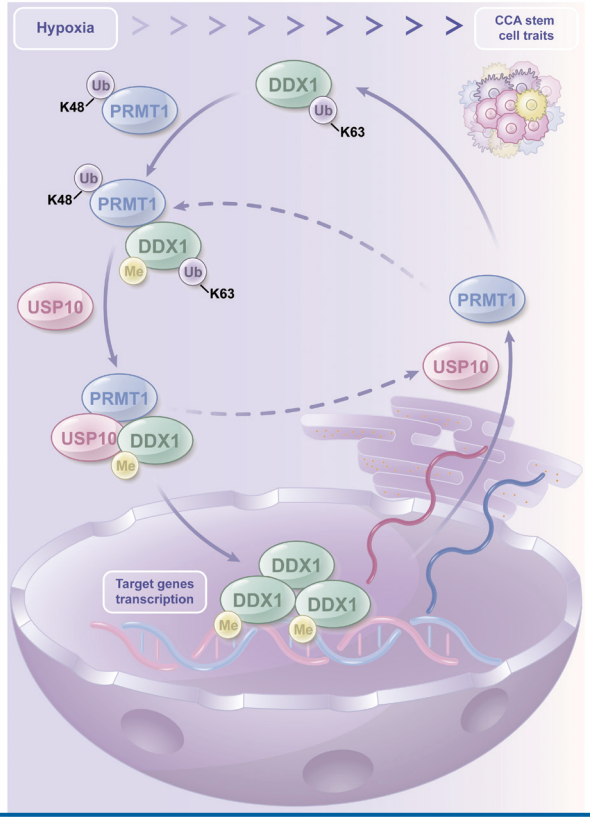

Study Highlights

- We identified PRMT1 as the methyltransferase for DDX1 R602 in CCA, whose modification is enhanced under hypoxia.
- The USP10-PRMT1-DDX1 feedback loop is formed via ADMA modification-mediated deubiquitination and nuclear translocation.
- GSK3368715 inhibits CCA progression in a DDX1 R602-ADMA–dependent manner, supporting its therapeutic potential.

Background/Aims: Cholangiocarcinoma (CCA) is a primary malignant neoplasm with an extremely poor prognosis. While combined chemoradiotherapy has been demonstrated to delay CCA progression to a certain extent, the absence of specific molecular biomarkers or targets significantly hinders the diagnosis and treatment of CCA.

Methods: Through cross-analysis of proteomics and ADMA modificationomics, we identified DDX1 overexpressed in CCA with elevated R602-ADMA modifications. HPLC-MS/MS identified PRMT1 as the methyltransferase and USP10 as the deubiquitinating enzyme for DDX1. Immunofluorescence and nuclear-cytoplasmic partitioning experiments confirmed DDX1's nuclear localization. GO and KEGG analyses clarify the biological functions of DDX1 in response to hypoxia. RNA-seq transcriptomics analyzed key pathways influenced by DDX1. A hydrodynamic in situ CCA mouse model was established to validate the chemopreventive effects of the PRMT1-specific inhibitor GSK715 on CCA development.

Results: DDX1 promotes CCA progression both in vivo and in vitro and can be inhibited by GSK715. Mechanistically, PRMT1 mediates ADMA modification at position R602 of DDX1. This modification promotes DDX1 nuclear localization by recruiting USP10 to deubiquitinate DDX1, while simultaneously inhibiting PRMT1 degradation. DDX1 promotes the transcription of PRMT1 and USP10 by binding to the mRNA 3'UTR region, establishing a positive feedback regulatory pathway. This mechanism promotes the occurrence and development of CCA and can serve as a target for the inhibitor GSK715 to suppress CCA progression.

Conclusions: Our study identified DDX1-R602-ADMA modification as a novel ADMA modification in CCA. It further confirmed its pivotal role in CCA progression. Targeting the USP10-PRMT1-DDX1 axis may represent a significant therapeutic approach for CCA. **(Clin Mol Hepatol 2026;32:843-865)**

Keywords: Cholangiocarcinoma; Arginine asymmetric dimethylation; Ubiquitination; PRMT1; DDX1

Corresponding author : Yongjun Chen
Division of Hepato-Pancreato-Biliary Surgery, Tongji Hospital, Tongji Medical College, Huazhong University of Science & Technology, Wuhan, Hubei 430030, P.R.China
Tel: +8602783665375, Fax: +86-027-83662640, E-mail: Yjchen@tjh.tjmu.edu.cn
https://orcid.org/0000-0002-4389-5399

Bing Wang
Division of Hepato-Pancreato-Biliary Surgery, Tongji Hospital, Tongji Medical College, Huazhong University of Science & Technology, Wuhan, Hubei 430030, P.R.China
Tel: +8602783665375, Fax: +86-027-83662640, E-mail: t0013008@aliyun.com
https://orcid.org/0000-0002-1533-6709

Feng Peng
Division of Hepato-Pancreato-Biliary Surgery, Tongji Hospital, Tongji Medical College, Huazhong University of Science & Technology, Wuhan, Hubei 430030, P.R.China
Tel: +8602783665375, Fax: +86-027-83662640, E-mail: fpeng@hust.edu.cn
https://orcid.org/0000-0002-7487-1752

*These authors contribute equally: Wenzheng Liu, Yangwei Liao, and Yiyang Kuai.

Editor: Terence Kin Wah Lee, The Hong Kong Polytechnic University, Hong Kong

Received: Nov. 8, 2025 / **Revised:** Jan. 20, 2026 / **Accepted:** Feb. 5, 2026

Abbreviations:

ADMA, asymmetric dimethylation; CCA, cholangiocarcinoma; CLIP, cross-linking immunoprecipitation; DIA, data-independent acquisition; GO, Gene Ontology; HPLC-MS/MS, high-performance liquid chromatography-mass spectrometry; KEGG, Kyoto Encyclopedia of Genes and Genomes; PTMs, post-translational modifications; sgRNA, single guide RNA

INTRODUCTION

Cholangiocarcinoma (CCA) is a malignant neoplasm originating from the epithelial cells of the biliary system.[1] Despite the presence of genetic heterogeneity, the common features of bile duct invasion and multipolar metastasis establish the biological commonality of the tumors.[2] On a global scale, the morbidity and mortality rates of CCA are increasing annually,[3] and specific molecular markers or targets are absent for the diagnosis and treatment of CCA.[4] Research has demonstrated a correlation between aberrant post-translational modifications (PTMs) of proteins and the development and progression of CCA.[5]

PTMs of non-histone proteins[6,7] play a critical role in various cellular processes.[8,9] Dysregulation of PTMs has been demonstrated to be a contributing factor to the development of cancer.[10,11] Recently, arginine methylation of non-histone proteins has been identified as a prevalent PTM catalyzed by arginine methyltransferases[12,13] and classified as monomethylation (MMA), symmetric dimethylation (SDMA), and asymmetric dimethylation (ADMA).[14,15] PRMT1 mediates over 75% of protein ADMA modifications, exhibiting distinct catalytic activities and substrate specificities across different diseases. GSK3368715 (GSK715) is a potent, reversible, S-adenosylmethionine (SAM)-noncompetitive inhibitor that binds to the protein substrate-binding pocket of PRMT1.[16] Methylation frequently impacts the binding of ubiquitin ligases or deubiquitinating enzymes to the substrate, thereby functioning as a regulatory "on/off switch" that governs the ubiquitination of the substrate and affects a variety of biological functions.[17,18] The intricate regulatory network that PTMs in tumor cells form makes elucidating the specific mechanisms of interactions between different PTMs targeting the same substrate a key scientific issue for PTM therapies in tumors.[19-21]

DDX1 is a DEAD-box RNA helicase and a key member of the RNA-binding protein (RBP) family.[22] As a crucial regulator of RNA metabolism,[23] DDX1 plays a vital role in controlling transcription and translation initiation,[24] as well as providing genomic protection in various solid tumours.[25] Although DDX1 is implicated in the pathogenesis of multiple cancers,[26] research on its role in CCA development remains limited to date.

This study provides a comprehensive elucidation of the mechanism by which ADMA of the R602 site on the DDX1 protein, facilitated by PRMT1 in CCA, promotes transcription of both PRMT1 and USP10 by recruiting USP10 to facilitate DDX1 nuclear translocation. USP10 enhances DDX1's R602-ADMA modification by stabilizing the PRMT1 protein, thereby establishing a dual positive feedback regulation mechanism that amplifies the stem-like characteristics of CCA cells during cancer progression. According to data-independent acquisition (DIA) quantitative proteomics and ADMA modification profiling analyses, DDX1 expression is elevated in CCA tissues, and ADMA modification at the R602 site increases under hypoxic conditions. High-performance liquid chromatography-mass spectrometry (HPLC-MS/MS) results indicate that DDX1's R602-ADMA modification is mediated by PRMT1 and recruits USP10. RNA sequencing and enrichment analysis findings reveal that DDX1 activates stemness pathways in CCA cells. Notably, both in vivo and in vitro experiments have demonstrated that the PRMT1-specific inhibitor GSK3368715 suppresses DDX1 nuclear translocation by inhibiting R602-ADMA modification of DDX1. Consequently, this results in the attenuation of stemness characteristics in CCA cells and the subsequent inhibition of CCA progression. This therapeutic approach may offer a viable strategy for treating CCA.

MATERIALS AND METHODS

Patient samples

Human CCA and paracancerous samples were obtained from the Department of Biliopancreatic Surgery, Tongji Hospital, Tongji Medical College, Huazhong University of Science and Technology. All studies related to clinical samples and data followed the principles of the Declaration of Helsinki and were approved by the Ethics Committee of Tongji Hospital (Approval No. SHYJS-CP-2001002). Patient details are presented in Supplementary Table 1.

In vivo experiments

C57BL/6 mice and BALB/c nude mice were purchased from Spearfish Biotechnology Co. (Beijing, China). The Laboratory Animal Welfare and Ethics Committee of Tongji Hospital, Tongji Medical College, Huazhong University of

Science and Technology, China, approved the animal studies (Approval No. TJH-202306014).

Mouse in situ CCA model

An in situ mouse CCA model was established using hydrodynamic tail vein injection and the Sleeping Beauty transposon.[27]

Subcutaneous xenograft tumor model

Six-week-old female BALB/c nude mice from Spearfish Biotechnology Co. were used. Cells were counted in advance according to the experimental grouping, 2×10^6 per mouse, and cells were resuspended in PBS.

Liver metastasis model

Six-week-old female BALB/c nude mice from Spearfish Biotechnology Co. were used. Cells were counted in advance according to the experimental grouping, 2×10^5 per mouse, and cells were resuspended in PBS. The following operations were performed in the operating room of the Laboratory Animal Center, and all instruments were sterilized. Ligation was performed in the center of the spleen, and the spleen was divided into proximal and distal ends with vascular tips. And 100 μL of cell suspension containing 2×10^5 cells was slowly injected into the proximal spleen. The mice were observed every two days, and their body weights were measured. When no weight gain was observed and the mice were depressed, the mice were executed, and the livers were fixed in 4% formaldehyde.

Plasmid construction, transfection, and lentivirus production

The total cDNA of CCA cells was used as the template, and the cDNA of DDX1, USP10, and PRMT1 was obtained by PCR. The polymerase used for PCR was 2×Phanta Flash Master Mix (P510, Vazyme, Nanjing, China).

The sequences of all primers used are summarized in Supplementary Table 2.

CRISPR cas9-mediated gene knockout

To construct DDX1 as well as PRMT1 knockout cell lines, we designed single guide RNA (sgRNA) targeting human DDX1 or PRMT1 and ligated it into the Px459 vector.

The specific sequences of the sgRNAs used in this section are shown in Supplementary Table 3.

Dual luciferase reporter assay

The 3'UTR, 5'UTR, and CDS sequences of USP10 and PRMT1 were obtained by PCR and cloned into a dual luciferase reporter vector. The following operations were performed in an environment protected from light using the Dual-Luciferase Reporter Assay Kit (DL101, Vazyme) according to the instructions.

Total RNA isolation, reverse transcription, and RT-qPCR

RNA extraction was performed using the TRIzol reagent (R701, Vazyme). Reverse transcription was performed using the reverse transcription kit HiScript II Q Select RT SuperMix for qPCR (+gDNA wiper) (R233-01, Vazyme). cDNA was obtained using 2 × Universal SYBR Green Fast qPCR Mix (RK21203, Abclonal, Wuhan, China) for RT-qPCR experiments as per instructions.

Primer sequences used in this section are shown in Supplementary Table 4.

Cross-linking immunoprecipitation (CLIP)

Cells were irradiated with a UV crosslinker at 260 nm and then lysed with 5× Cell Lysis Buffer (G2002, Servicebio, Wuhan, China) and Protease Inhibitor Cocktail (20138ES05, Yeasen, Shanghai, China). After the addition of 10 mg/mL RNaseA (G3405, Servicebio), and digested at room temperature for 15 minutes, DDX1 antibody and A/G magnetic beads (HY-K0202, MedChemExpress, Monmouth Junction, NJ, USA) were added, and the cells were incubated at 4°C overnight. The immunocomplexes were eluted with 50 mM Tris-HCl solution (pH=7.8) at 60°C. Reverse transcription of the RNA to cDNA was performed and analyzed by RT-qPCR.

GST pull-down assay

Bacteria were lysed with GST lysis buffer (50 mM Tris-HCl, pH 7.4, 0.5% NP-40, 1 mM EDTA, 150 mM NaCl, and protease inhibitor cocktail) and sonicated to obtain the GST

https://doi.org/10.3350/cmh.2025.1252

fusion proteins. The GST fusion proteins and cytosolic proteins were incubated with GST antibody and A/G magnetic beads at 4°C overnight. The next day, the cells were washed three times and boiled with 2× loading buffer for 15 minutes before being used for immunoblotting analysis.

Immunofluorescence staining

Cells were fixed in 4% formaldehyde, permeabilized with 0.1% Triton X-100 for 10 minutes, and blocked with 5% BSA. Primary antibodies were incubated with the cells overnight at 4°C. The following procedures were performed in a light-proof environment. The next day, coverslips were incubated with the secondary antibodies at 37°C for 2 hours. The nuclei were stained with DAPI.

Flow cytometry

Cells were digested with trypsin and obtained a cell suspension, which was incubated with a fluorescently labeled primary antibody for 30 minutes at room temperature. Cell viability was assessed by the Zombie Aqua Fixable Viability Kit (423101, Biolegend, San Diego, CA, USA). The stained cells were analyzed by flow cytometry using a BD FACSCelesta (423102, BD Biosciences, Franklin Lakes, NJ, USA) instrument and FlowJo software (TreeStar, Ashland, OR, USA). Antibodies used in this section are listed in Antibodies and Chemicals.

Tumor cell spheroid formation assay

CCA cells were inoculated in ultra-low adsorption dishes, and special medium for tumorsphere growth was prepared by adding B27 (1:50, Invitrogen, Carlsbad, CA, USA), human recombinant EGF (20 ng/mL, Sigma-Aldrich, St. Louis, MO, USA), bFGF (20 ng/mL, Sigma-Aldrich), and insulin (5 μg/mL, Sigma-Aldrich) to DMEM/F12 medium.

DIA relative quantitative proteomics analysis

After protein extraction and quantification, peptides were desalted using a C18 cartridge following FASP enzymatic digestion and then freeze-dried under vacuum. Each sample underwent DIA analysis with a screening threshold of Q value≤0.01. All mass spectrometry data were merged using Spectronaut software (version 19, Biognosys AG, Schlieren, Switzerland) to complete database searching of DIA mass spectrometry data and quantitative analysis of proteins via DIA. The database used was uniprotkb-Homo sapiens (Human) [9606]-205092-20250414.fasta, sourced from https://www.uniprot.org/taxonomy/9606.

Arginine methylation proteomics

In addition to Section *DIA Relative Quantitative Proteomics Analysis* incorporates asymmetric dimethylated peptide enrichment and differential analysis of asymmetric dimethylated arginine sites.

HPLC-MS/MS

HPLC-MS/MS sequencing was conducted with the assistance of Shanghai Omicsspace Biotech Co., Ltd. (Shanghai, China). HPLC-MS/MS analysis was performed on an Orbitrap Exploris 480 mass spectrometer coupled to a nano-HPLC interface (Dionex UltiMate 3000 nano HPLC, Thermo Scientific, Bremen, Germany).

RNA sequencing and enrichment analysis

Enrichment analysis was based on the principle of hypergeometric distribution, and clusterProfiler software was used to perform Gene Ontology (GO) (http://www.geneontology.org/), Kyoto Encyclopedia of Genes and Genomes (KEGG) (http://www.kegg.jp/), and Reactome pathway enrichment analyses on the differential gene sets.

Antibodies and chemicals

The DDX1-R602me2a rabbit polyclonal antibody was prepared by ABclonal (https://abclonal.com.cn).

The following other small-molecule materials were used: GSK3368715 dihydrochloride (HY-128717A, MedChemExpress); AMI-1 free acid (HY-18962A, MedChemExpress).

Detailed information on the antibodies is provided in Supplementary Table 5.

Statistical analyses

Statistical analysis was performed using GraphPad Prism

10 (GraphPad Software, La Jolla, CA, USA). Each experiment was repeated at least three times. Data were expressed as mean±standard deviation (SD). Two-factor analysis of variance (ANOVA) or two-tailed unpaired *t*-test was used. Survival curves were analyzed using the Kaplan–Meier method and the log-rank test. *P*-values less than 0.05 were considered statistically significant, and *P*-values were expressed as follows: **P*<0.05, ***P*<0.01, and ****P*<0.001. On the contrary, *P*-values equal to or greater than 0.05 were not statistically significant.

RESULTS

ADMA modification of R602 in DDX1 is elevated in CCA and correlates with hypoxic environments

To identify proteins highly expressed in CCA, quantitative proteomic sequencing was performed on tissue samples from three pathologically confirmed CCA patients paired with adjacent non-cancerous tissue. Functional annotation and enrichment analysis revealed the response to hypoxia (Supplementary Fig. 1A–C). Furthermore, multiple studies have confirmed that hypoxia induction has been proven to be a critical intervention condition in cancer research.[28,29] In order to identify the key proteins involved in hypoxia-induced elevation of ADMA in CCA, TFK-1 cells were cultured under hypoxic conditions and then subjected to modified proteomics sequencing (Fig. 1A). The cross-analysis of the 17 proteomics-upregulated results with the 9 modificationomics-upregulated results revealed asymmetric dimethylation at arginine 602 (R602) of the DDX1 peptide (Fig. 1B, C). A DDX1-R602-specific ADMA antibody (DDX1-R602-ADMA) was engineered and utilized to specifically detect DDX1-R602 ADMA through dot blotting (Supplementary Fig. 1D). Analysis of the amino acid sequence homology revealed that R602 is highly conserved throughout evolution (Fig. 1D). IHC staining of CCA tissue microarrays demonstrated that the expression of DDX1 and R602-ADMA was significantly elevated in CCA tissues compared with paracarcinoma tissues (*P*<0.01) (Fig. 1E, Supplementary Fig. 1E). The protein and R602-ADMA levels of DDX1 can be increased in a hypoxic environment and in response to the increasing Ado-Met concentration or the arginine methylation inhibitor AMI-1 (Supplementary Fig. 1F–I). Upon converting all intracellular DDX1 to the R602K mutant, hypoxia no longer increased ADMA modification of DDX1 (Fig. 1F, Supplementary Fig. 1J). The above results confirm that ADMA modification at the R602 site of DDX1 is elevated in CCA and correlates with hypoxic environments.

The asymmetric dimethylation modification of arginine in DDX1-R602 is mediated by PRMT1 and enhanced by hypoxia

To identify the arginine-modifying enzyme of DDX1, arginine methyltransferase 1 (PRMT1) was found after HPLC-MS/MS (Fig. 2A). Further experiments and molecular docking confirmed the direct combination of DDX1 and PRMT1 between the PRMT1d1 fragment and the DDX1F2 fragment (Fig. 2B, C, Supplementary Fig. 2A–C). Moreover, under hypoxic conditions, PRMT1 accumulates more DDX1 (Supplementary Fig. 2D). Immunofluorescence staining revealed that DDX1 and PRMT1 exhibit binding interactions with each other within both the nucleus and cytoplasm (Fig. 2D). R602-ADMA modification of DDX1 positively correlates with PRMT1 expression and correlates with its methyltransferase activity. This was confirmed in cell experiments using the PRMT1-specific inhibitor GSK3368715 (GSK715) and in PRMT1 knockout (PRMT1KO) cells (Fig. 2E, Supplementary Fig. 2E–H). The hypoxia-induced expression of DDX1 in CCA and the elevated ADMA modification levels are similarly correlated with the methyl transfer activity of PRMT1 and the R602 site (Fig. 2F, Supplementary Fig. 2I–L). It indicates that PRMT1-mediated ADMA modification at the DDX1R602 site is crucial for the elevated expression of DDX1 in CCA.

USP10 is recruited by ADMA modification of arginine at position 602 of DDX1 and promotes DDX1 nuclear localization, while also stabilizing the PRMT1 protein

To investigate the impact of ADMA modification on the intracellular function of DDX1's R602 residue, further GO and KEGG functional annotation and enrichment analysis were performed on the cross-results from proteomics and ADMA modification profiling. The results indicate that the majority of the enriched biological processes (BP) are as-

https://doi.org/10.3350/cmh.2025.1252

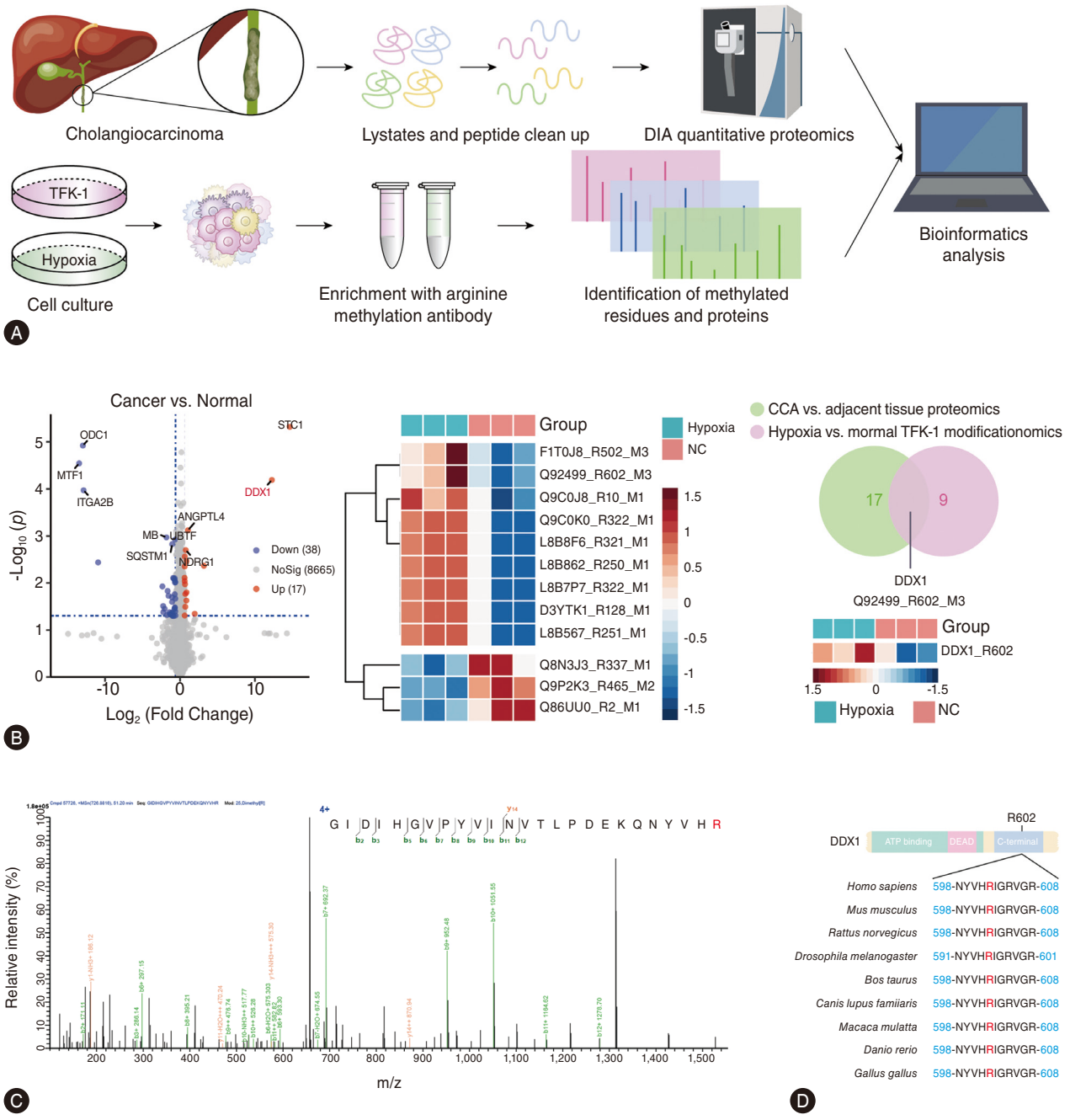

Figure 1. DDX1-R602-ADMA is hypoxically induced and overexpressed in CCA. (A) Flowchart of sample processing and data analysis for proteomics and ADMA-modified proteomics. (B) Proteomics volcano plot. ADMA modification proteomics heatmap. Venn diagram of proteins upregulated in proteomics and ADMA-modified proteomics, with heatmaps displayed after removal of proteomic background noise. (C) Secondary mass spectrum of the DDX1R602 ADMA. (D) Homology alignment of the DDX1-R602 across different species. (E) IHC staining of human CCA TMAs for DDX1-R602-ADMA and scoring. Data were presented as means±SD. (F) R602-ADMA modification levels were measured in DDX1 or DDX1-R602K cells with or without hypoxia induction. ***P*<0.01. ADMA, asymmetric demethylation; CCA, cholangiocarcinoma; DIA, data-independent acquisition; ECC, extrahepatic cholangiocarcinoma; IHC, Immunohistochemistry; TMAs, tissue microarrays; WT, wild-type.

sociated with mRNA and nucleic acid metabolism within the nucleus (Fig. 3A). Multiple studies indicate that protein methylation often interacts with other PTMs to jointly influence protein degradation or intracellular localization. Analysis of

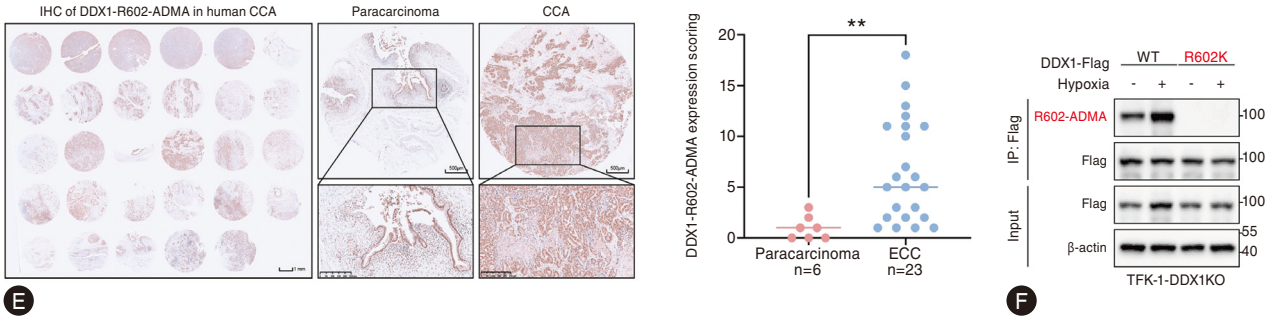

Figure 1. Continued.

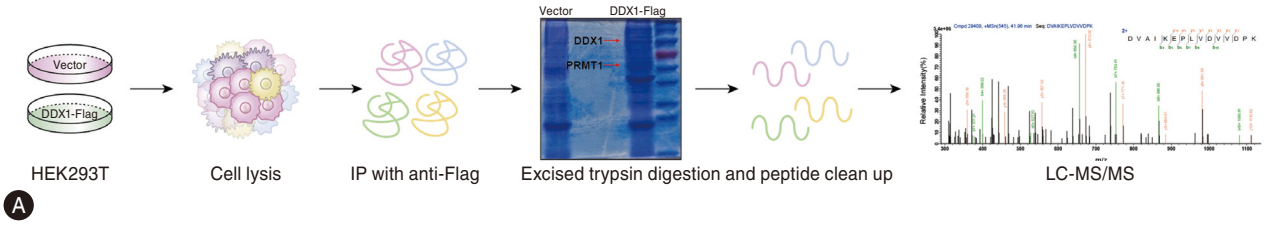

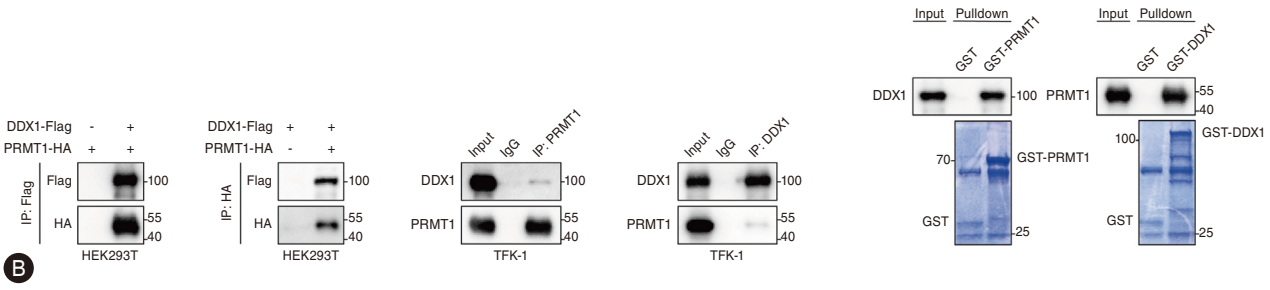

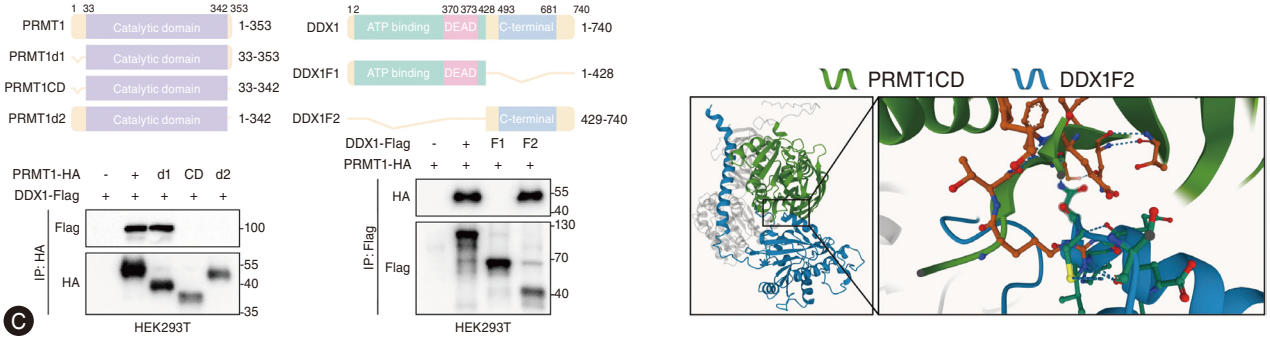

Figure 2. PRMT1 acts as the arginine methyltransferase for DDX1, and ADMA mediates the increased expression of DDX1 in CCA. (A) Flowchart of sample processing for HPLC-MS/MS sequencing of DDX1-binding proteins and secondary mass spectrum of PRMT1. (B) Co-IP and GST pull-down of DDX1 and PRMT1. (C) Co-IP with truncated mutants of PRMT1 or DDX1. Computer-performed molecular docking simulation of DDX1 with PRMT1. (D) Immunofluorescence staining of PRMT1 (red) and DDX1 (green). Line intensity maps show co-localization of PRMT1 and DDX1 (n=5). (E) PRMT1 gradient increase, mutation, GSK715 detection of R602-ADMA modification level in DDX1. (F) Detection of the effects of hypoxia on PRMT1-mediated increased DDX1 expression and enhanced R602-ADMA modification. ADMA, asymmetric demethylation; CCA, cholangiocarcinoma; Co-IP, Co-immunoprecipitation; DMSO, dimethyl sulfoxide; HPLC-MS/MS, high-performance liquid chromatography-mass spectrometry; WT, wild-type.

DDX1 HPLC-MS/MS results drew our attention to the deubiquitinating enzyme USP10 (Fig. 3B). After validating the interaction between USP10 and DDX1 (Supplementary Fig. 3A–D), intracellular immunofluorescence colocalization analysis

https://doi.org/10.3350/cmh.2025.1252

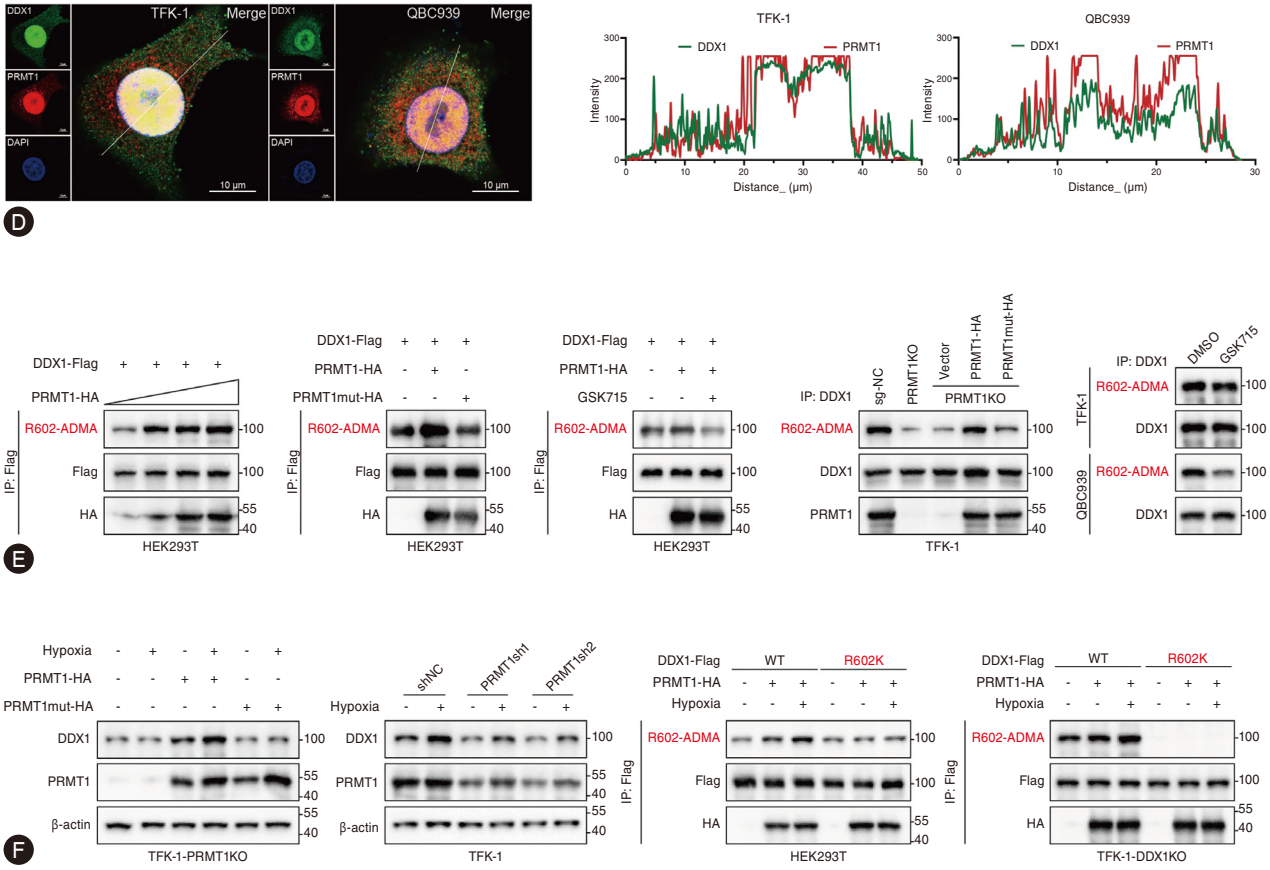

Figure 2. Continued.

vrevealed that USP10 primarily associates with DDX1 in the cytoplasm (Fig. 3C). Molecular docking was employed to simulate the binding of USP10 to the DDX1 protein (Fig. 3D). USP10 catalytic inactivation plasmids (USP10C424A, USP10mut) confirmed the catalytic deubiquitination effect of USP10 on DDX1 (Supplementary Fig. 3E). We further determine the relationship between ADMA modification and the deubiquitination of DDX1. R602-ADMA modification enhances the deubiquitination of DDX1 by USP10, whereas PRMT1 itself does not exert this effect (Fig. 3E). Hypoxia also enhances the deubiquitinating activity of USP10, which correlates with the DDX1R602 site (Fig. 3F, Supplementary Fig. 3F, G). The results demonstrate that hypoxia exerts a comparable effect on the recruitment of USP10, facilitated by ADMA modification at the DDX1R602 site.

USP10 mediates K63 deubiquitination of DDX1 (Supplementary Fig. 4A), which is often associated with the intracellular localization of proteins. DDX1 is progressively transported into the nucleus as intracellular USP10 levels increase, and hypoxia enhances this process (Fig. 4A, Supplementary Fig. 4B–D). PRMT1 and hypoxia both enhance USP10-mediated nuclear localization of DDX1 through R602 ADMA modification of DDX1 (Fig. 4B, Supplementary Fig. 4E, F). In exploring the enhancing effect of PRMT1 on USP10-mediated deubiquitination of DDX1, we discovered that USP10 itself exhibits a certain degree of enhancing effect on ADMA modification of DDX1 R602 (Fig. 3E). HPLC-MS/MS analysis of the PRMT1 and further experiments discovered that PRMT1 and USP10 interact within cells (Fig. 4C, Supplementary Fig. 5A–F). USP10 attenuates PRMT1 ubiquitinylation via the K48 pathway (Supplementary Fig. 5F, G), not only inhibiting PRMT1 protein degradation but also enhancing PRMT1's methyltransferase activity (Fig. 4E, F, Supplementary Fig. 5H–K).

We have thus identified a positive feedback loop involving PTMs of DDX1: PRMT1 catalyzes ADMA modification

 https://doi.org/10.3350/cmh.2025.1252

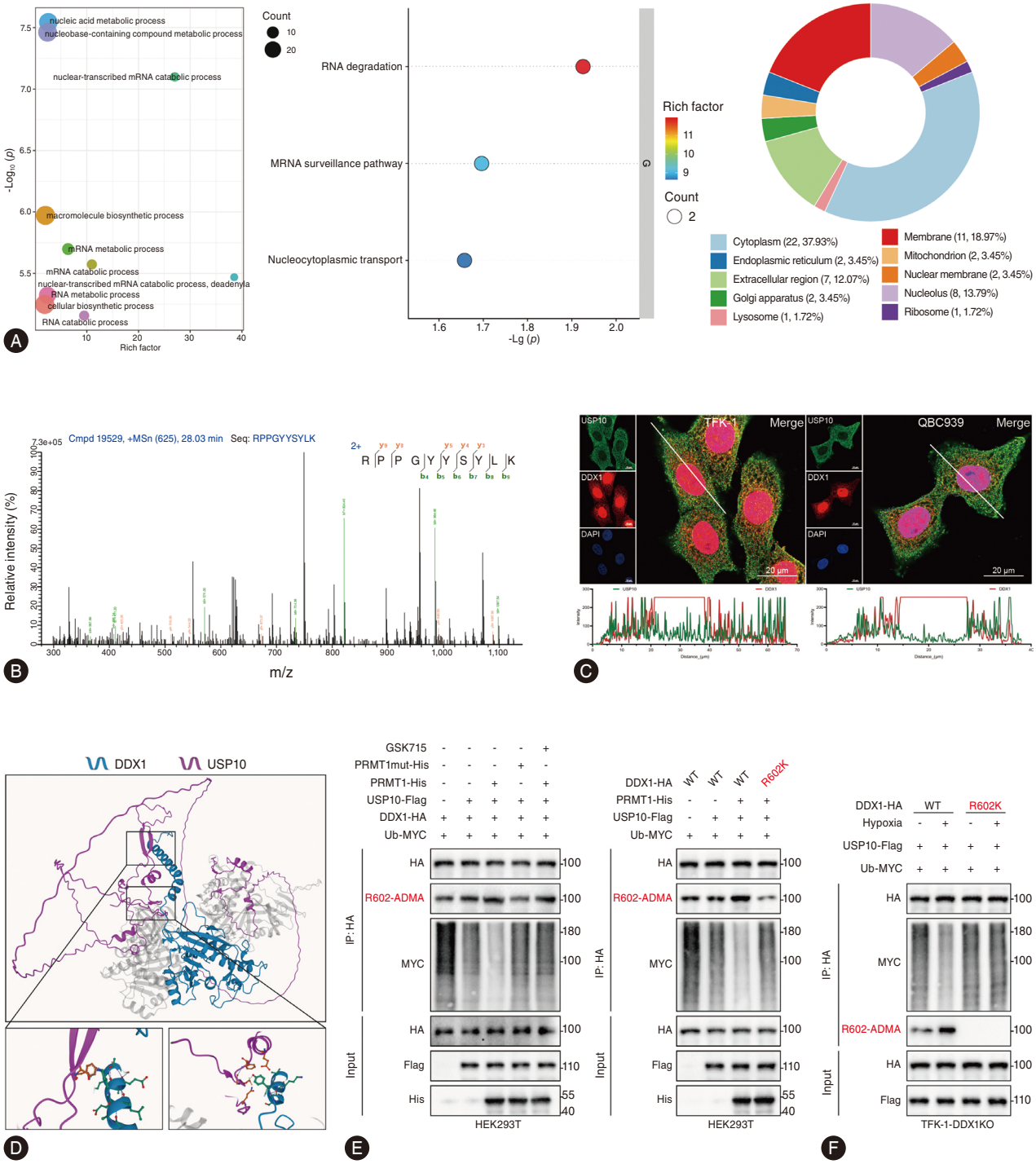

Figure 3. USP10 binds to DDX1, and its deubiquitinating activity on DDX1 is enhanced by PRMT1-mediated DDX1 R602-ADMA modification. (A) After removing protein background through proteomics and ADMA modificationomics cross-analysis, all proteins underwent GO enrichment analysis. Functional enrichment analysis of annotation results was performed using Fisher's exact test algorithm. Results are presented as *P*-values, with values below 0.05 indicating significant functional enrichment. Annotation and statistical analysis of cellular components (CC, subcellular localization) in the GO database. (B) Secondary mass spectrometry spectrum of the USP10 peptide segment binding to the DDX1 protein. (C) Confocal microscopy observation of immunofluorescence staining of USP10 (green) and DDX1 (red). Images represent at least n=5 imaged cells. (D) Computer-performed molecular docking simulation of DDX1 with PRMT1. (E) Detection of the enhancing effect of R602-ADMA modification on deubiquitination. (F) The role of ADMA modification in R602 in enhancing deubiquitination under hypoxia. ADMA, asymmetric demethylation; GO, Gene Ontology; WT, wild-type.

https://doi.org/10.3350/cmh.2025.1252

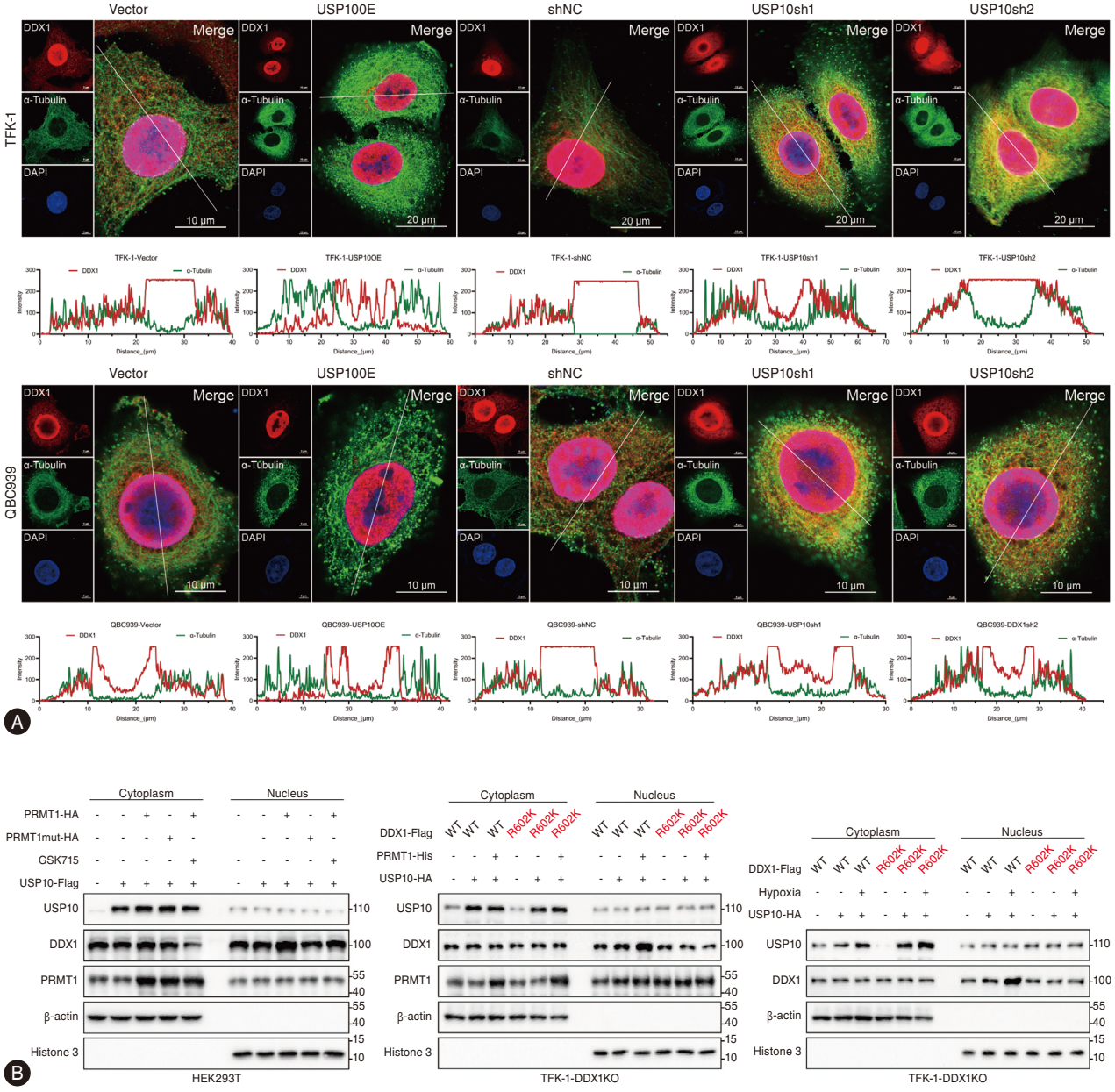

Figure 4. USP10 mediates DDX1 nuclear transport and enhances ADMA modification at the DDX1 R602 site by stabilizing the PRMT1 protein. (A) Immunofluorescence staining of DDX1 (red) and cytoplasmic marker α-Tubulin (green) was observed by confocal microscopy. Line intensity maps show co-localization of cytoplasmic and DDX1. Images represent at least n=5 imaged cells. (B) Detection of the role of PRMT1's methyltransferase activity and DDX1-R602's ADMA modification in USP10-mediated DDX1 nuclear translocation. (C) Secondary mass spectrometry spectrum of the USP10 peptide segment binding to the PRMT1 protein. (D) Computer-performed molecular docking simulation of DDX1 with PRMT1. (E) Effect of USP10 on PRMT1 protein levels. (F) The effect of USP10 on the level of R602-ADMA modification of DDX1 mediated by PRMT1. ADMA, asymmetric demethylation; WT, wild-type.

at the R602 site of DDX1, which in turn recruits USP10 to catalyze DDX1 deubiquitination. Concurrently, USP10 binds to PRMT1 and stabilizes the PRMT1 protein, thereby enhancing PRMT1's R602-ADMA modification of DDX1 and recruiting additional USP10 molecules.

DDX1 promotes a positive feedback loop by binding to the 3' UTR region of mRNA to facilitate PRMT1 and USP10 transcription

To elucidate the function of DDX1 upon nuclear localiza-

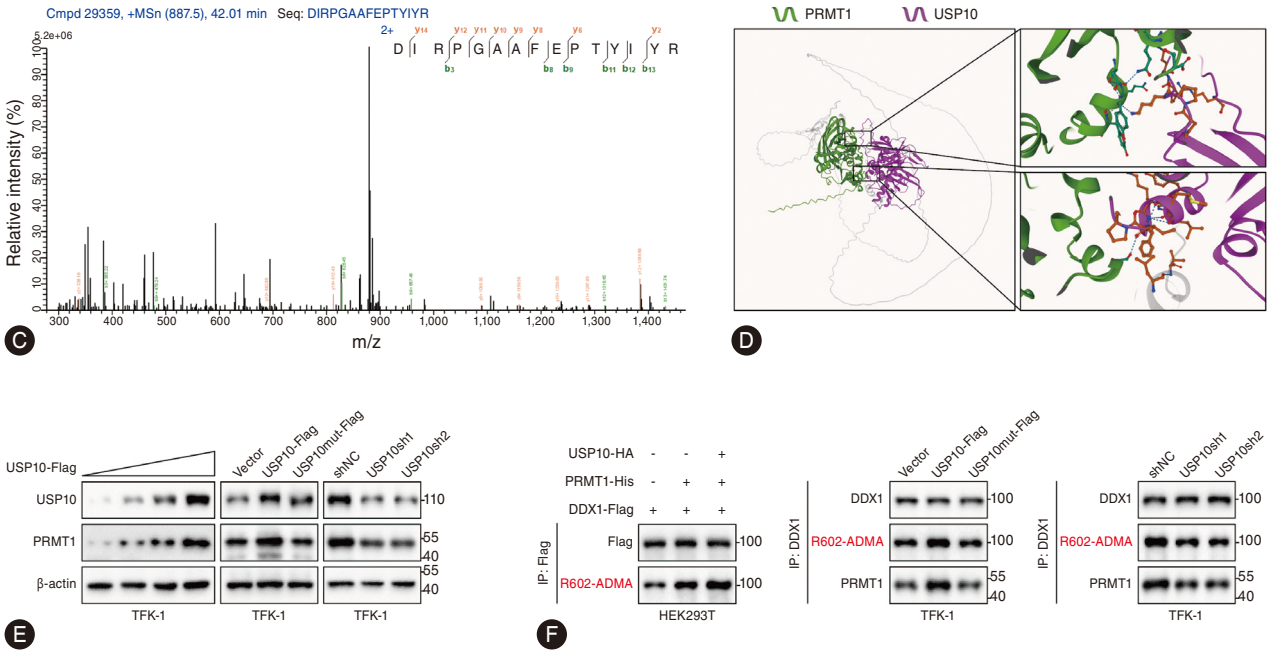

Figure 4. Continued.

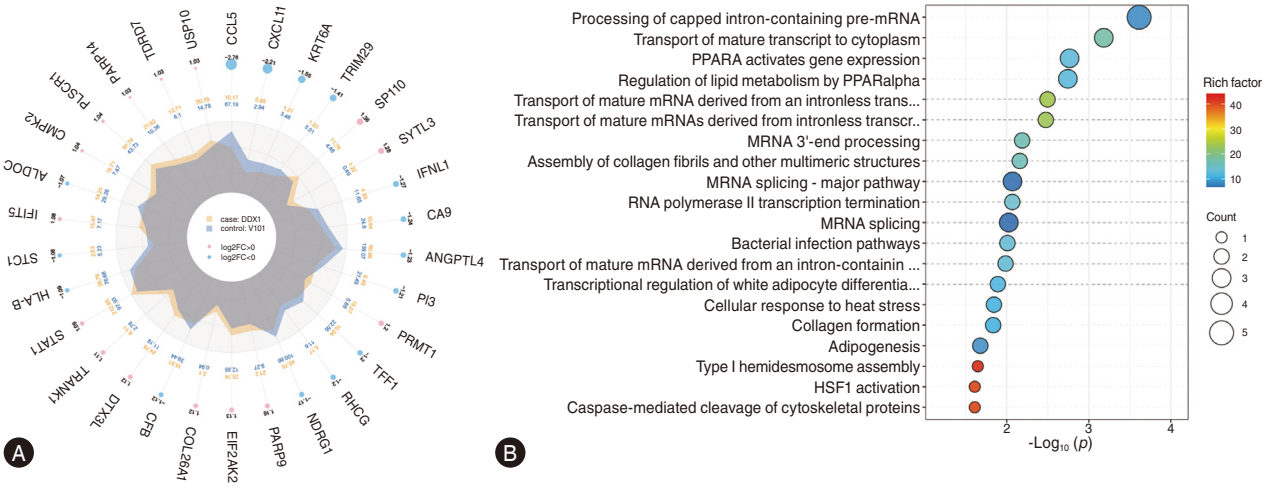

Figure 5. DDX1 binds to the 3' UTR regions of PRMT1 and USP10 mRNA to promote transcription. (A) Radar chart of differential gene expression levels between DDX1OE and V101 in RNA-seq sequencing. (B) Differentially expressed genes reactome pathway analysis. (C) The luciferase reporter gene detects changes in fluorescence intensity when DDX1 acts on different structures of USP10 and PRMT1 mRNAs. (D) The luciferase reporter gene detects changes in fluorescence intensity upon overexpression or knockdown of DDX1 acting on the 3'UTR region of USP10 and PRMT1 mRNA. (E) Effect of PRMT1 on USP10 protein levels. (F) Detection of the role of the R602 site in PRMT1 on USP10 mRNA and protein levels. ***P*<0.01 and ****P*<0.001; ns, not significant. WT, wild-type.

tion in CCA, we performed RNA sequencing and revealed that both USP10 and PRMT1 were upregulated by DDX1 expression (Fig. 5A, Supplementary Fig. 6A). Reactome pathway annotation revealed strong associations with mRNA processing (Fig. 5B). CLIP and dual luciferase reporter assays revealed that DDX1 exerted its effect on the 3'UTR region of mRNAs and that the signal intensity exhibited a positive correlation with DDX1 content (Fig. 5C, D, Supplementary Fig. 6B, C). PRMT1 could positively affect the USP10 content and correlate with its catalytic activity (Fig. 6E, Supplementary Fig. 6D). USP10 was unable to affect the mRNA or protein expression of USP10 in the ab-

https://doi.org/10.3350/cmh.2025.1252

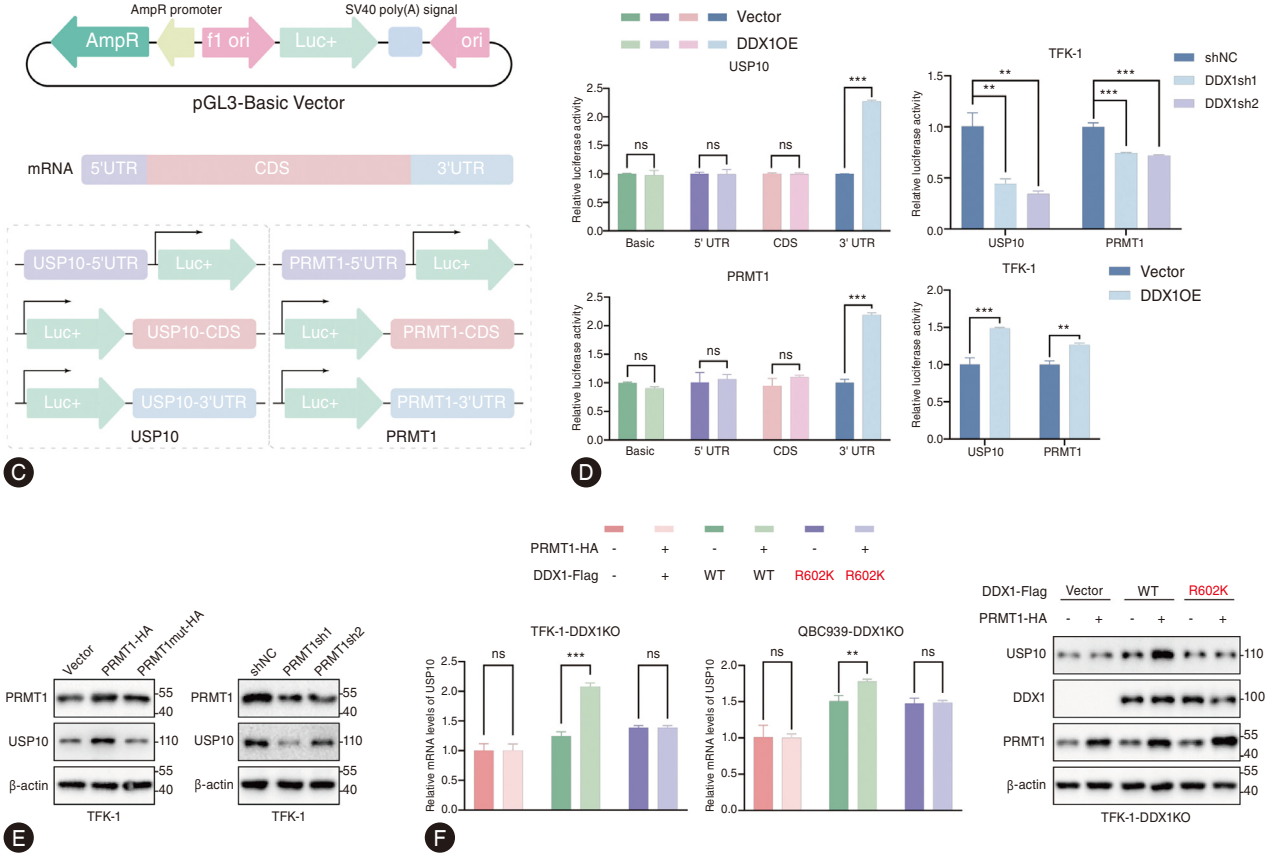

Figure 5. Continued.

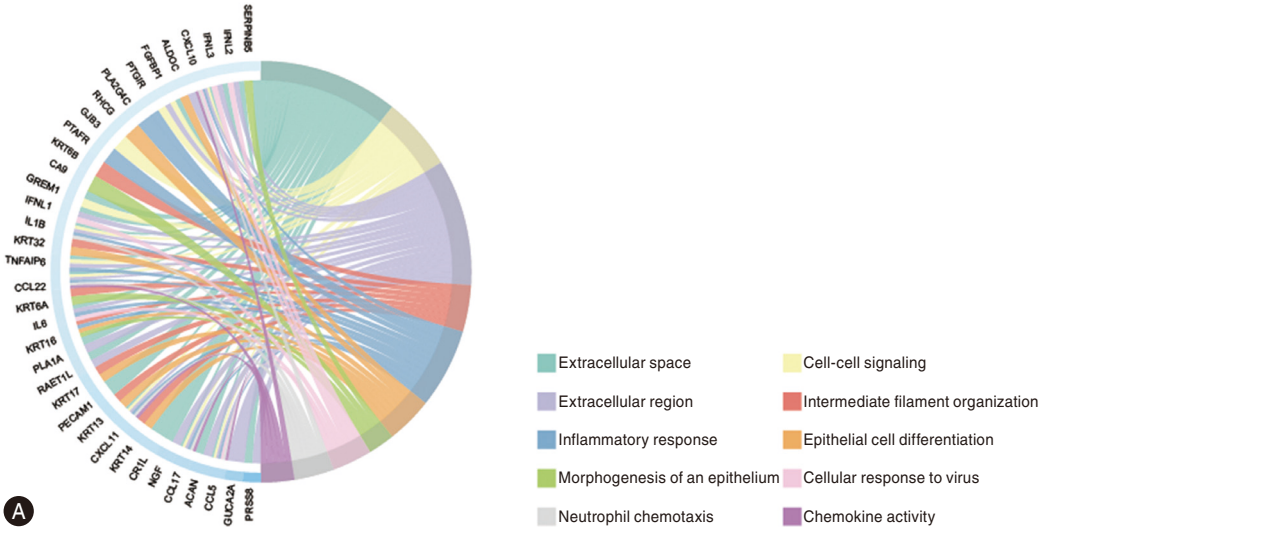

Figure 6. DDX1 promotes CCA progression. (A) Perform GO enrichment analysis on differentially expressed genes from RNA-seq to characterize their functions. (B, C) Subcutaneous xenograft tumor experiments, statistical analysis of volume and weight changes, and immunohistochemical Ki67 staining. (D) Spleen injection liver metastasis experiment and statistical analysis of the number of metastatic foci. (E) Representative images of tumor spheres formed by TFK-1 cells after DDX1 overexpression or knockdown and statistical plots of tumor sphere size (n=3). (F) CCA cell pluripotency markers after DDX1 overexpression or knockdown. (G) CCA cell surface stemness marker positivity rate after DDX1 overexpression or knockdown. **P*<0.05, ***P*<0.01, and ****P*<0.001. CCA, cholangiocarcinoma; GO, Gene Ontology.

 https://doi.org/10.3350/cmh.2025.1252

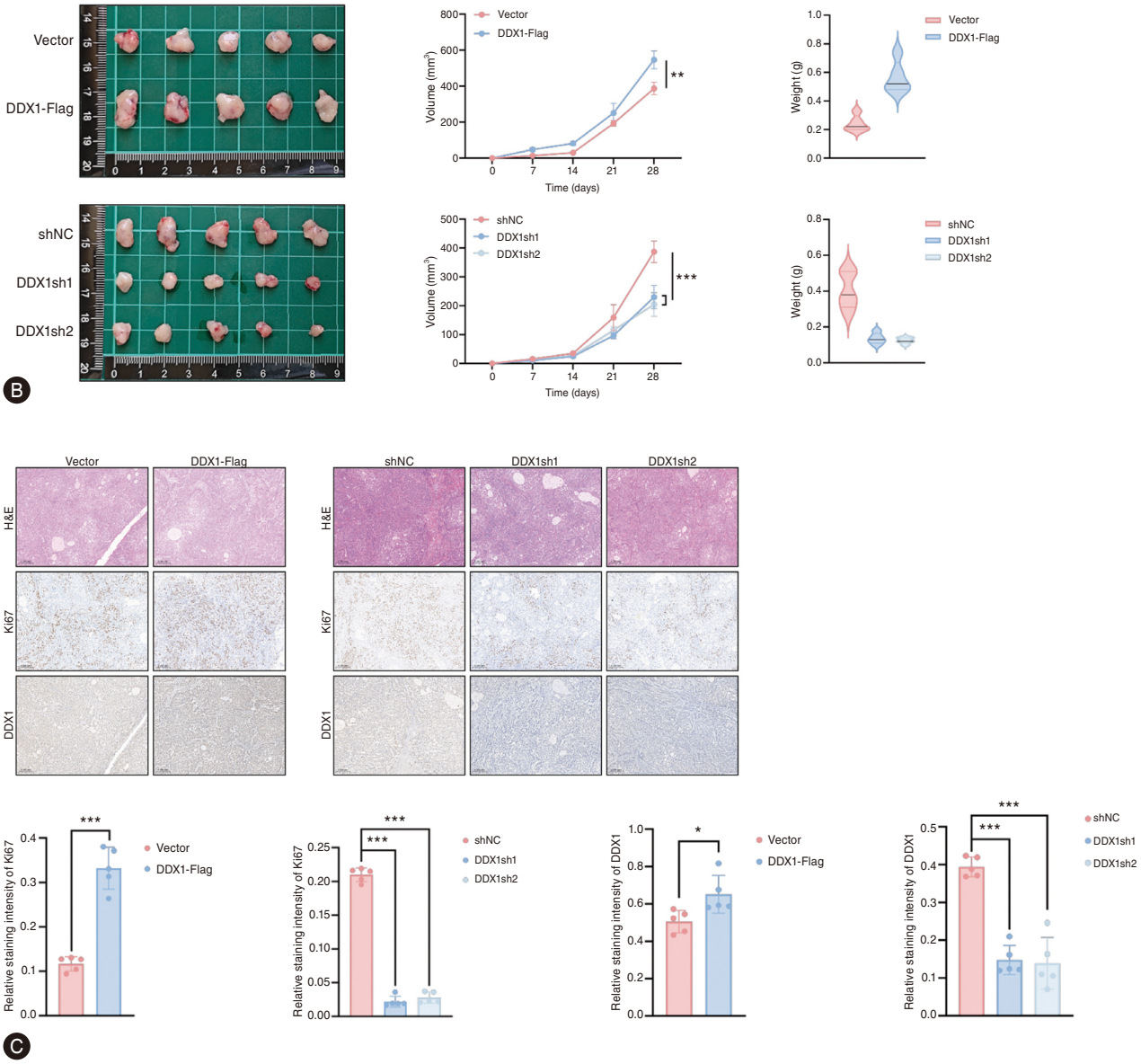

Figure 6. Continued.

sence of ADMA modification of DDX1 (Fig. 6F).

Our experiments established a USP10-PRMT1-DDX1 positive feedback network. PRMT1 catalyzes ADMA modification of DDX1, which recruits USP10. USP10 simultaneously mediates DDX1 deubiquitination and nuclear translocation while deubiquitinating PRMT1 to enhance its protein stability, thereby further elevating DDX1's ADMA modification levels. Upon entering the nucleus, DDX1 binds to the mRNA of PRMT1 and USP10, promoting transcription and thereby triggering positive feedback regulation of PRMT1 and USP10 protein levels.

GSK715 suppresses CCA stem cell characteristics and inhibits CCA progression by inhibiting DDX1R602's ADMA modification through PRMT1 inhibition

Following the discovery of DDX1 overexpression in CCA through proteomics, we further investigated the impact of DDX1 on the development and progression of CCA. GO

https://doi.org/10.3350/cmh.2025.1252

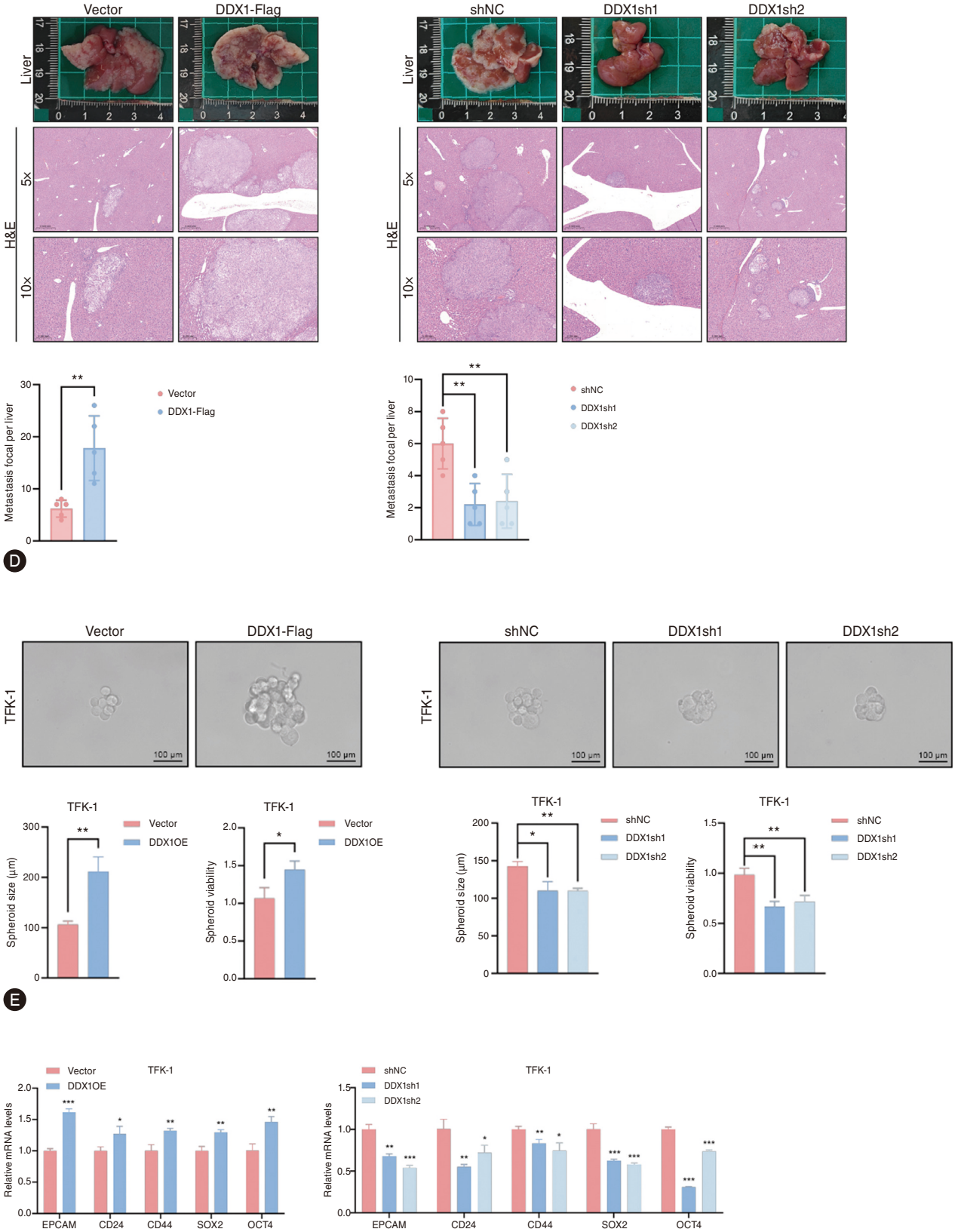

Figure 6. Continued.

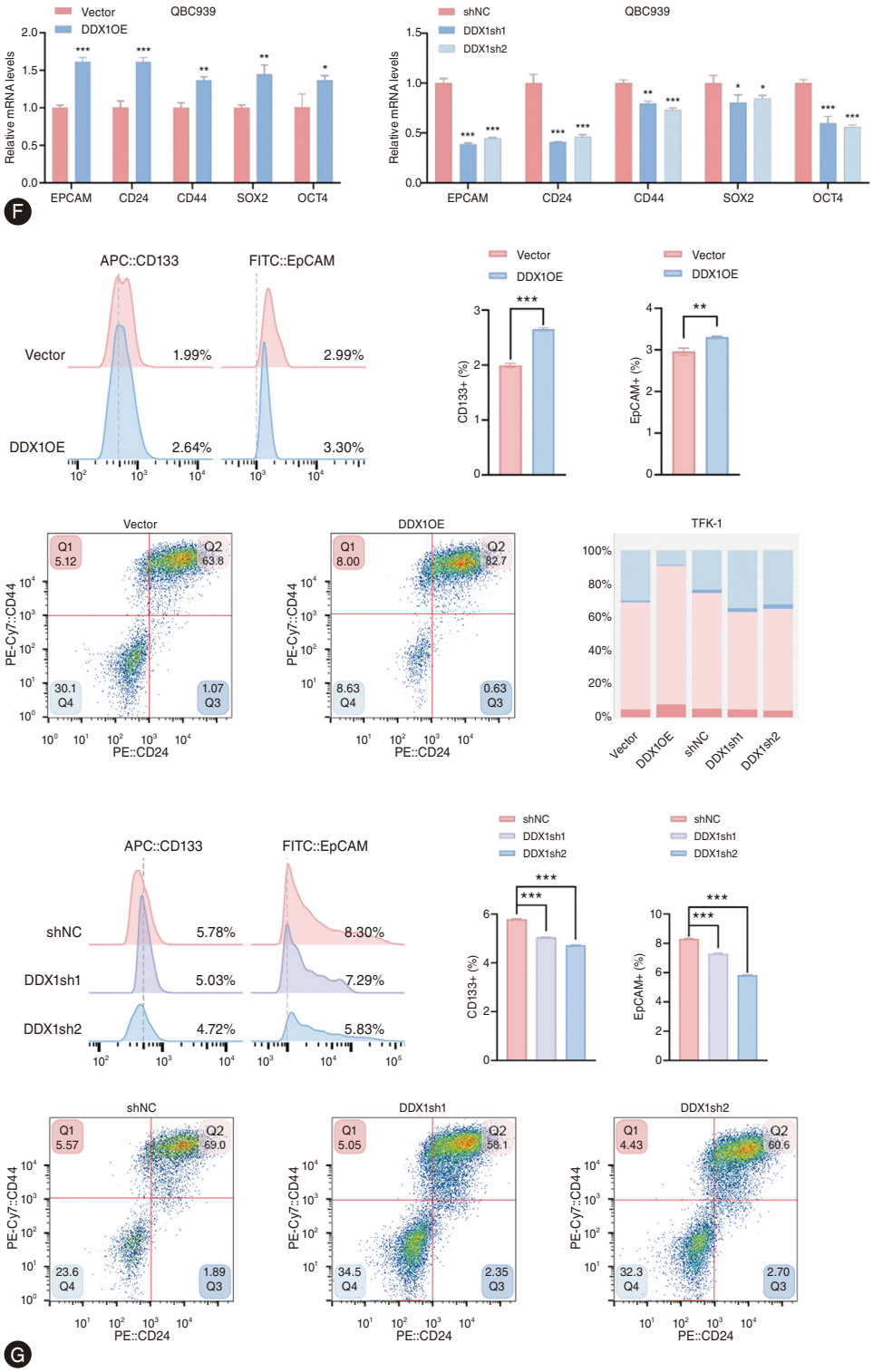

Figure 6. Continued.

analysis on RNA-seq data identified epithelial cell differentiation-related pathways (Fig. 6A). After confirming in vitro that TFK-1 cell proliferation rate positively correlates with DDX1 expression (Supplementary Fig. 7A), xenograft ex-

https://doi.org/10.3350/cmh.2025.1252

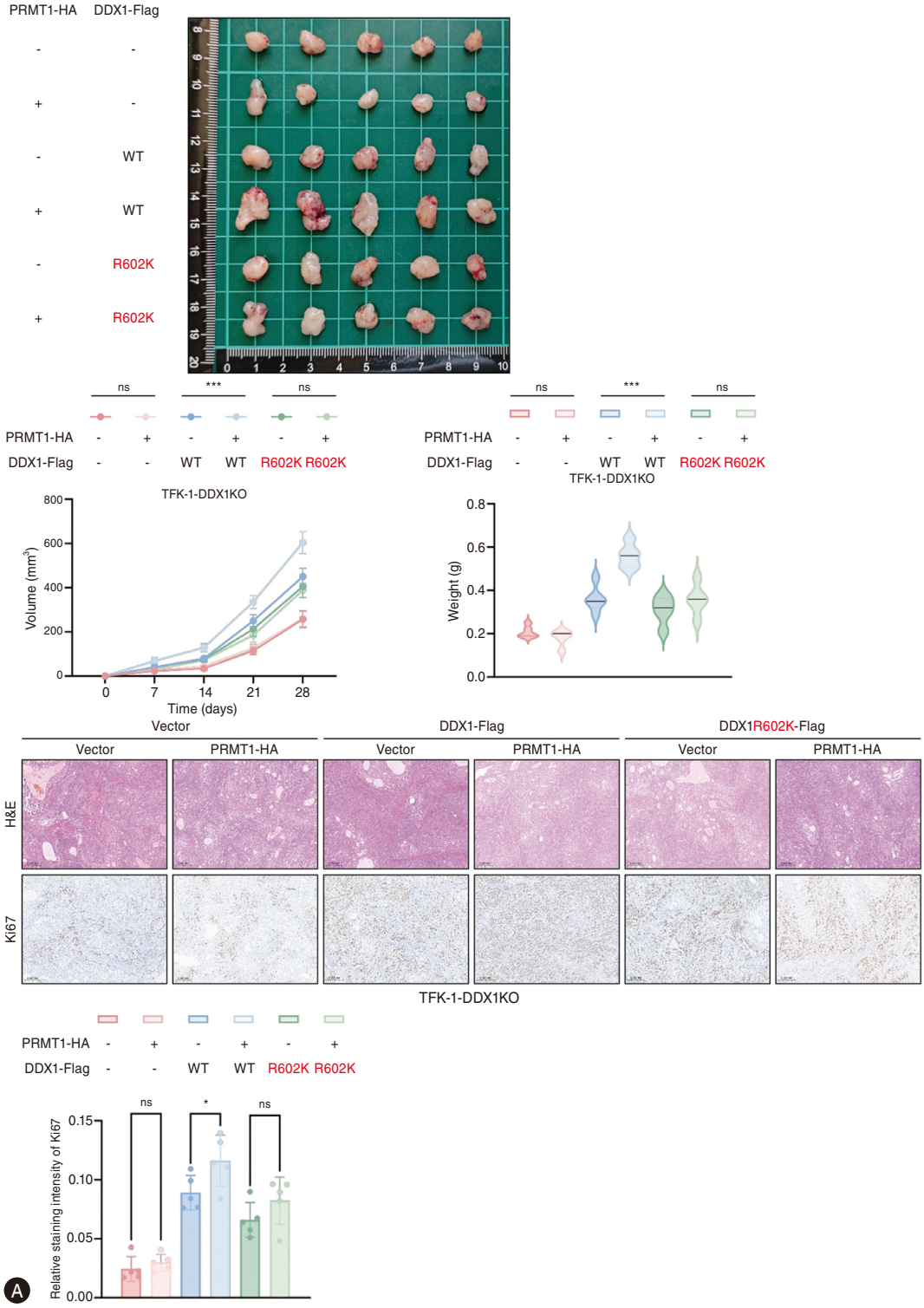

Figure 7. GSK715 inhibits CCA progression. (A) Subcutaneous xenograft tumor experiments, statistical analysis of volume and weight changes, and immunohistochemical Ki67 staining. (B) Spleen injection liver metastasis experiment and statistical analysis of the number of metastatic foci. (C) CCK-8 assay and colony formation assay were used to evaluate the effect of GSK715 on TFK-1 cell proliferation. (D) Transwell assays were conducted to evaluate the effects of GSK715 on the invasion and migration of TFK-1 cells. (E) Evaluating the therapeutic efficacy of GSK715 against CCA in a mouse CCA model. *P<0.05, **P<0.01, and ***P<0.001; ns, not significant. ALT, alanine aminotransferase; AST, aspartate aminotransferase; CCA, cholangiocarcinoma; DMSO, dimethyl sulfoxide; WT, wild-type.

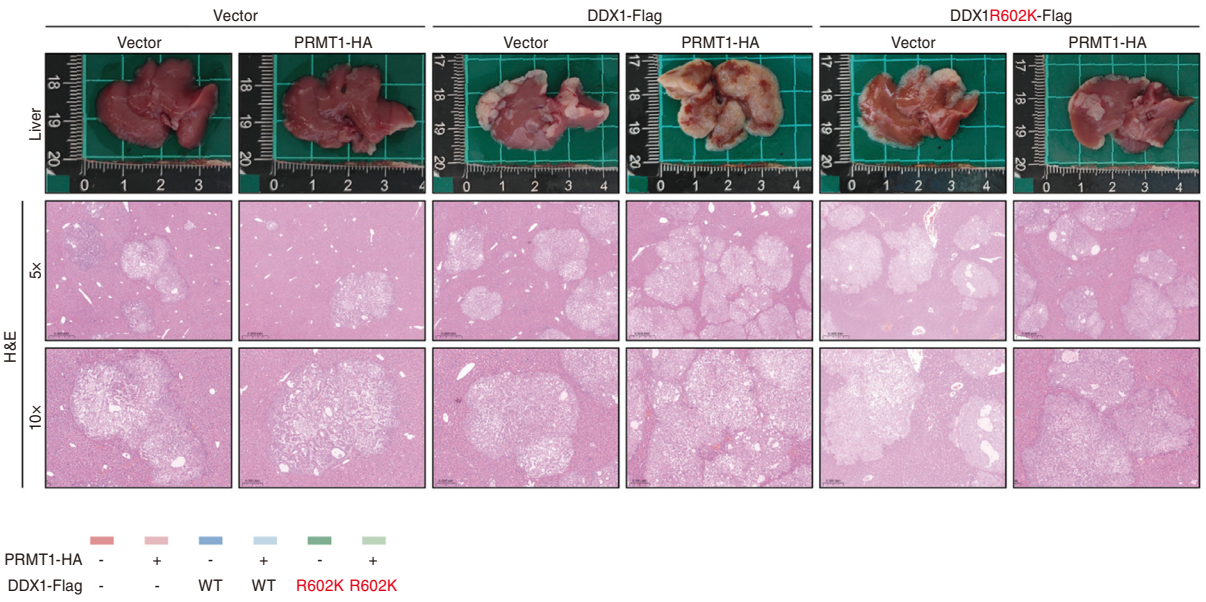

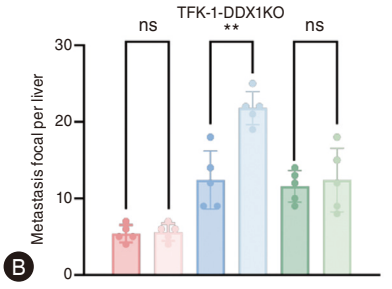

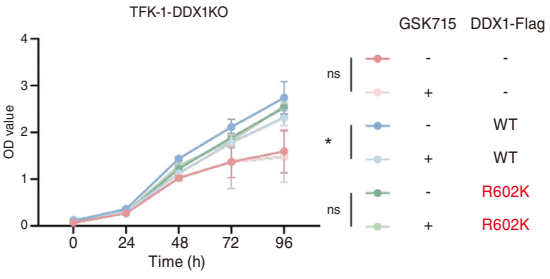

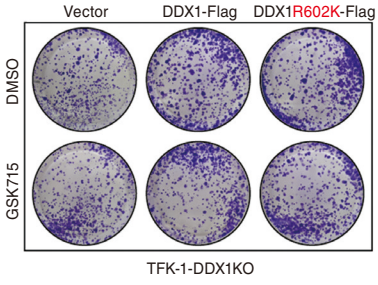

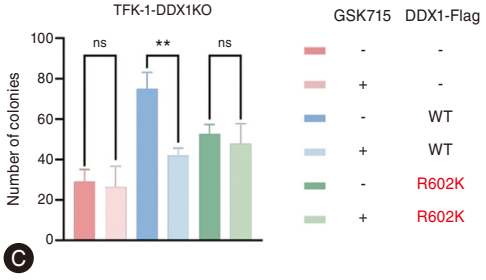

Figure 7. Continued.

https://doi.org/10.3350/cmh.2025.1252

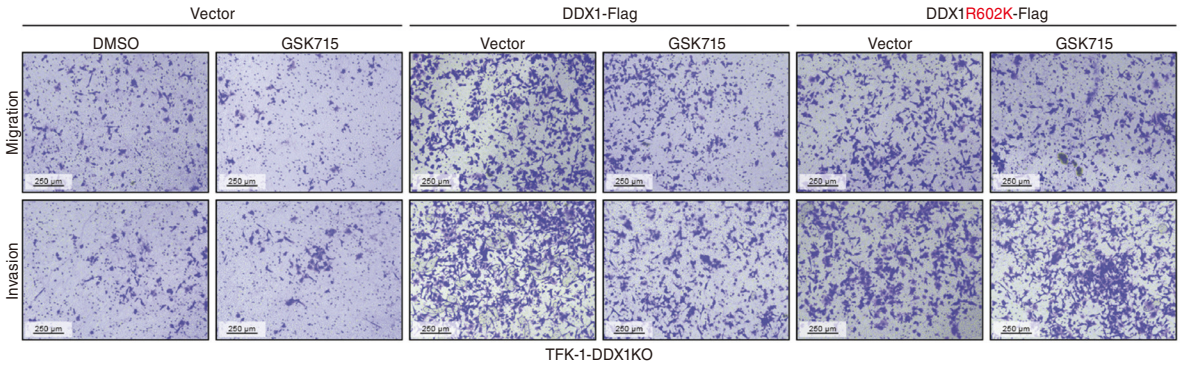

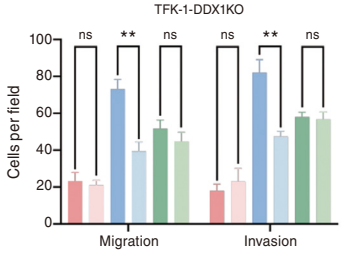

D

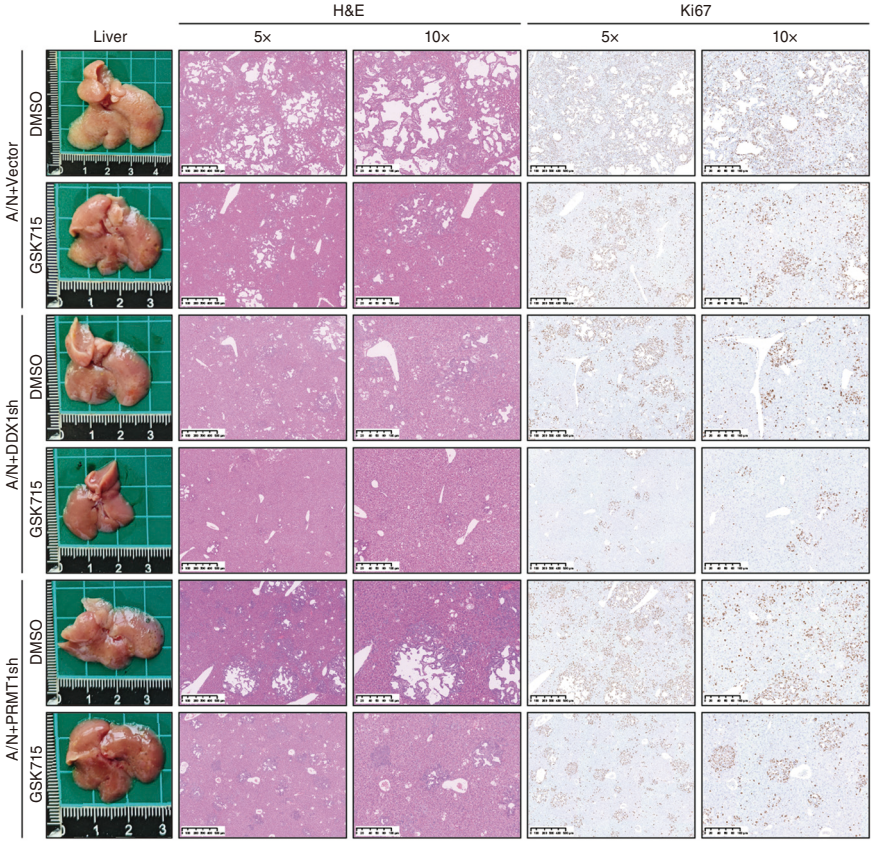

Figure 7. Continued.

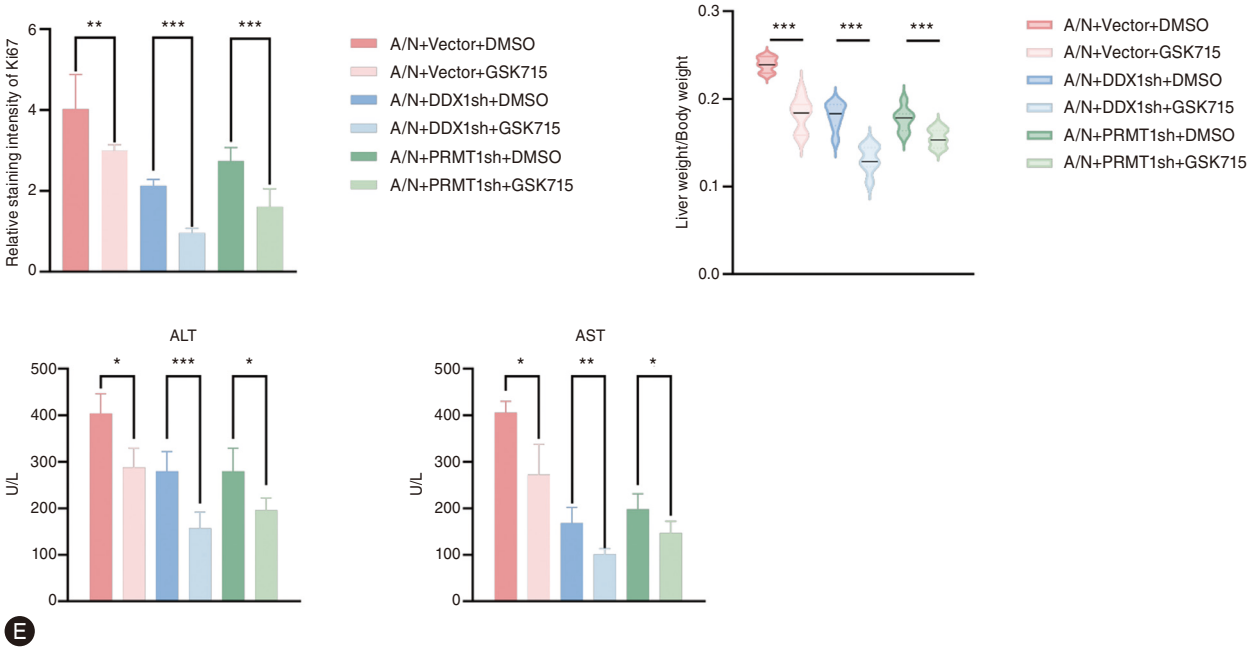

Figure 7. Continued.

periments in nude mice demonstrated that DDX1 similarly promotes tumor cell proliferation in vivo (Fig. 6B, C). Transwell invasion and migration assays, along with liver metastasis experiments via spleen injection in nude mice, demonstrated that DDX1 enhances TFK-1 cell migration both in vivo and in vitro (Supplementary Fig. 7B, Fig. 6D). These experimental results suggest the potential of DDX1 as a therapeutic target for CCA. As DDX1 has been demonstrated to play a pivotal role in the development of CCA both in vivo and in vitro, we established wild-type and DDX1-overexpressing or knockdown in situ CCA models in C57BL/6 mice. The progression rate of liver cancer in mice is also positively correlated with DDX1 expression (Supplementary Fig. 7C). This validated the role of DDX1 in CCA initiation and progression. As demonstrated in prior research, the elimination of DDX1 has been observed to impact the stem cell characteristics of cancerous cells.[30,31] The results demonstrated that TFK-1 cells overexpressing DDX1 formed tumor spheres with significantly increased diameters (Fig. 6E) and led to a substantial increase in the expression levels of stem cell-associated nuclear transcription factors (EpCAM, CD24, CD44, SOX2, and OCT4).[2,32] DDX1 overexpression significantly augmented cell membrane CD133 and EpCAM enrichment and increased the proportion of $CD24^{+}CD44^{+}$ cells (Fig. 6F).

Mechanistic experiments have demonstrated that PRMT1-mediated ADMA modification at R602 of DDX1 is critical for DDX1 function. Phenotypic studies further confirm that PRMT1-enhanced CCA cell stemness similarly depends on R602 ADMA modification (Supplementary Fig. 8A, B), while PRMT1 also promotes CCA progression both in vivo and in vitro (Fig. 7A, B, Supplementary Fig. 8C–E). We further investigated whether the PRMT1-specific inhibitor GSK715 could suppress CCA progression. The results demonstrated that GSK715 inhibited the formation of tumor spheres in the presence of the methylation site of DDX1 and reduced the membrane surface stemness markers and the proportion of $CD24^{+}CD44^{+}$ cells in CCA cells (Supplementary Fig. 9A, B). Following in vitro experiments confirming that GSK715 inhibits proliferation and invasion in TFK-1 cells (Fig. 7C, D), we generated mouse models of CCA with wild-type expression and with DDX1 or PRMT1 specifically inhibited. These models were then treated with intraperitoneal injections of GSK715 to evaluate its in vivo efficacy in suppressing CCA progression. Results showed that while GSK715 exhibited limited tumor progression inhibition in wild-type CCA mouse models, its therapeutic efficacy was significantly enhanced when DDX1 or PRMT1 expression was suppressed (Fig. 7E). This finding provides a theoretical basis for incorporating DDX1 inhibitor combination therapy

https://doi.org/10.3350/cmh.2025.1252

in subsequent experiments.

In summary, GSK715 has been demonstrated to impede the progression of CCA and mitigate liver injury to a certain extent by selectively inhibiting DDX1-R602ADMA.

DISCUSSION

PTM of proteins is a critical factor in tumor development,[33,34] exerting its influence through multiple mechanisms.[35,36] The study of multiple PTMs targeting proteins that play key roles has emerged as a promising avenue for cancer therapy.[37,38]

Our experimental findings elucidated the interplay between two PTMs of DDX1 in CCA, unveiling a positive feedback network. Cross-referencing proteomics and modificationomics results revealed the R602-ADMA modification of DDX1. HPLC-MS/MS analysis of DDX1-binding proteins revealed that PRMT1 mediates DDX1-R602-ADMA modification and USP10 mediates DDX1 deubiquitination and promotes DDX1 nuclear localization. The deubiquitination of DDX1 is not only enhanced by ADMA modification of DDX1-R602 but also correlates with hypoxic conditions. HPLC-MS/MS analysis of PRMT1-binding proteins revealed that USP10 stabilizes the PRMT1 protein, thereby amplifying ADMA modification and further intensifying USP10 recruitment. This positive feedback pathway confirms the central role of DDX1 R602 ADMA modification and elucidates the relationship between the two PTMs of DDX1 in detail.

To elucidate the biological function of DDX1 in CCA, RNA-seq was performed, and found that DDX1 upregulates the transcription of PRMT1 and USP10 by binding to the 3' UTR region of mRNA. This elucidates a positive feedback relationship between DDX1 PTM and transcription. GO enrichment analysis of RNA-seq revealed that DDX1 upregulates the epithelial cell differentiation pathway. Inhibition of ADMA modification at DDX1R602 by GSK715 effectively weakened the stem-like characteristics of CCA cells and suppressed cancer progression in CCA mice. This finding provides a theoretical basis and feasible approach for targeted therapy in CCA.

In summary, we identified two PTM modifications of DDX1 under hypoxic conditions and established the central role of the R602-ADMA modification, which serves as a survival-related prognostic indicator for CCA and may represent a potential therapeutic target for its treatment.

Authors' Contribution

W.L. and Y.L. designed the experiments; W.L., Y.L., and Y.K. performed most of the experiments with the assistance of X.G., J.C., J.L., J.S., X.Y., and J.Z.; W.L. and Y.C. wrote and edited the manuscript; Y.C. provided funding support for the project; X.G., J.C., J.L., J.S., X.Y., Y.K., S.H., Z.Z., B.W., F.P. and J.Z. performed data analysis and supervised the project. All authors read and approved the final paper.

Acknowledgements

The authors would like to express their sincerest gratitude to the Experimental Medicine Center of Tongji Hospital, Tongji Medical School, Huazhong University of Science and Technology, for providing invaluable equipment support for immunofluorescence experiments.

This work was supported by grants from the National Natural Science Foundation of China (Grant No. #82173069 and #82573911 to Y.C.), Key Research and Development Program of Hubei Province (Grant No. #2024BCB054 to Y.C.).

Conflicts of Interest

The authors have no conflicts to disclose.

SUPPLEMENTARY MATERIAL

Supplementary material is available at Clinical and Molecular Hepatology website (http://www.e-cmh.org).

REFERENCES

1. Mizumoto M, Shibuya K, Terashima K, Murakami M, Murakami M, Shioyama Y, et al. Particle therapy for intrahepatic cholangiocarcinoma: a multicenter prospective registry study, systematic review and meta-analysis. Liver Cancer 2025;14:211-222.
2. Wang Q, Long T, Tang P, Xu C, Wang L, Liu J, et al. Metabolic reprogramming in cholangiocarcinoma cancer stem cells: emerging therapeutic paradigms. Cancer Lett 2025;622:217714.

3. Vithayathil M, Khan SA. Current epidemiology of cholangiocarcinoma in Western countries. J Hepatol 2022;77:1690-1698.
4. Niu M, Ding WX. Overcoming drug resistance by harnessing mitochondrial divisome for treating cholangiocarcinoma. J Hepatol 2025;83:835-837.
5. Yang L, Niu K, Wang J, Shen W, Jiang R, Liu L, et al. Nucleolin lactylation contributes to intrahepatic cholangiocarcinoma pathogenesis via RNA splicing regulation of MADD. J Hepatol 2024;81:651-666.
6. Masclef L, Ahmed O, Estavoyer B, Larrivée B, Labrecque N, Nijnik A, et al. Roles and mechanisms of BAP1 deubiquitinase in tumor suppression. Cell Death Differ 2021;28:606-625.
7. Guan C, Gao J, Zou X, Shi W, Hao Y, Ge Y, et al. A novel 167-amino acid protein encoded by CircPCSK6 inhibits intrahepatic cholangiocarcinoma progression via IKBα ubiquitination. Adv Sci (Weinh) 2025;12:e2409173.
8. Liu C, Wang X, Li Q, Gao X, Zeng K, Li B, et al. Apolipoprotein E promotes primary resistance to AR-targeted therapy via inducing TRIM25-mediated AR ubiquitination and sensitizes immunotherapy in prostate cancer. Theranostics 2025;15:5572-5591.
9. Yan Y, Yu J, Wang W, Xu Y, Tison K, Xiao R, et al. Palmitoylation prevents B7-H4 lysosomal degradation sustaining tumor immune evasion. Nat Commun 2025;16:4254.
10. Zhang N, Sun L, Zhou S, Ji C, Cui T, Chu Q, et al. Cholangiocarcinoma PDHA1 succinylation suppresses macrophage antigen presentation via alpha-ketoglutaric acid accumulation. Nat Commun 2025;16:3177.
11. Dai P, Sun Y, Huang Z, Liu YT, Gao M, Liu HM, et al. USP2 inhibition unleashes CD47-restrained phagocytosis and enhances anti-tumor immunity. Nat Commun 2025;16:4564.
12. Sun M, Qiao Z, Wei S, Liang Z, Zhang L, Jiang B, et al. Global methylation profiling by selective release of methylated sites from immobilized tryptic peptides. Anal Chem 2025;97:9620-9626.
13. Liu S, Zhang W, Liu W, Ding Z, Zhang R, Han Y, et al. PRMT1-mediated SWI/SNF complex recruitment via SMARCC1 drives IGF2BP2 transcription to enhance carboplatin resistance in head and neck squamous cell carcinoma. Adv Sci (Weinh) 2025;12:e2417460.
14. Walton J, Ng ASN, Arevalo K, Apostoli A, Meens J, Karamboulas C, et al. PRMT1 inhibition perturbs RNA metabolism and induces DNA damage in clear cell renal cell carcinoma. Nat Commun 2024;15:8232.
15. Wang X, Jin J, Yan H, Liu J, Huang S, Bai H, et al. The mRNA export pathway licenses viral mimicry response and antitumor immunity by actively exporting nuclear retroelement transcripts. Sci Transl Med 2025;17:eado4370.
16. Nicholson TB, Chen T, Richard S. The physiological and pathophysiological role of PRMT1-mediated protein arginine methylation. Pharmacol Res 2009;60:466-474.
17. Dong Z, She X, Ma J, Chen Q, Gao Y, Chen R, et al. The E3 ligase NEDD4L prevents colorectal cancer liver metastasis via degradation of PRMT5 to inhibit the AKT/mTOR signaling pathway. Adv Sci (Weinh) 2025;12:e2504704.
18. Wu Y, Qin X, Xiang M, Deng J. PRMT1 upregulates SIRT6 by enhancing arginine methylation of E2F7 to inhibit vascular smooth muscle cell senescence in aortic dissection. FASEB J 2025;39:e70579.
19. Yang X, Liu Y, Cao J, Wu C, Tang L, Bian W, et al. Targeting epigenetic and post-translational modifications of NRF2: key regulatory factors in disease treatment. Cell Death Discov 2025;11:189.
20. Ma HY, Sun R, Tian T, Zhou XJ, Chen ZH, Cao XC, et al. NFIX suppresses breast cancer cell proliferation by delaying mitosis through downregulation of CDK1 expression. Cell Death Discov 2025;11:77.
21. Oyon D, Lopez-Pascual A, Castello-Uribe B, Uriarte I, Orsi G, Llorente S, et al. Targeting of the G9a, DNMT1 and UHRF1 epigenetic complex as an effective strategy against pancreatic ductal adenocarcinoma. J Exp Clin Cancer Res 2025;44:13.
22. Wang Y, Yasmin L, Li L, Gao P, Xu X, Sun X, et al. DDX1 vesicles control calcium-dependent mitochondrial activity in mouse embryos. Nat Commun 2022;13:3794.
23. Suzuki T, Takagi S, Funada J, Egawa Y, Yamakawa M, Hara T, et al. DDX1 is required for non-spliceosomal splicing of tRNAs but not of XBP1 mRNA. Commun Biol 2025;8:92.
24. Li Z, Zhou M, Cai Z, Liu H, Zhong W, Hao Q, et al. RNA-binding protein DDX1 is responsible for fatty acid-mediated repression of insulin translation. Nucleic Acids Res 2018;46:12052-12066.
25. Zhu D, Liang H, Tong B, Du Z, Li G, Zhang W, et al. DDX1 methylation mediated MATR3 splicing regulates intervertebral disc degeneration by initiating chromatin reprogramming. Nat Commun 2025;16:6153.
26. Gao B, Li X, Li S, Wang S, Wu J, Li J, et al. Pan-cancer analysis identifies RNA helicase DDX1 as a prognostic marker. Phenomics 2022;2:33-49.
27. Di-Luoffo M, Pirenne S, Saandi T, Loriot A, Gérard C, Dauguet N, et al. A mouse model of cholangiocarcinoma

https://doi.org/10.3350/cmh.2025.1252

uncovers a role for Tensin-4 in tumor progression. Hepatology 2021;74:1445-1460.
28. Collet L, Ardin M, Venet D, Berthet J, Ghamry-Barrin S, Treilleux I, et al. Unraveling the tumor microenvironment and PD-L1 expression across tissue types in high-grade serous ovarian cancer in the NeoPembrOV/GINECO phase II randomized trial. Clin Cancer Res 2025;31:3317-3331.
29. Shepherd STC, Kelly-Morland C, Drage S, Brady AF, Macwana R, Pickering L, et al. Fatal intracranial haemorrhage shortly after belzutifan initiation in von Hippel-Lindau (VHL) disease-associated haemangioblastoma. ESMO Open 2025;10:105109.
30. Yang Q, Xu P, Liu Q, Hu F, Xie X, Jiang L, et al. Depleting DDX1 sensitizes non-small cell lung cancer cells to chemotherapy by attenuating cancer stem cell traits. Life Sci 2023;323:121592.
31. Wang F, He J, Liu S, Gao A, Yang L, Sun G, et al. A comprehensive RNA editome reveals that edited Azin1 partners with DDX1 to enable hematopoietic stem cell differentiation. Blood 2021;138:1939-1952.
32. Giron-Michel J, Padelli M, Oberlin E, Guenou H, Duclos-Vallée JC. State-of-the-art liver cancer organoids: modeling cancer stem cell heterogeneity for personalized treatment. BioDrugs 2025;39:237-260.
33. Ko PJ, Dixon SJ. Protein palmitoylation and cancer. EMBO Rep 2018;19:e46666.
34. Li Y, Zhang R, Hei H. Advances in post-translational modifications of proteins and cancer immunotherapy. Front Immunol 2023;14:1229397.
35. Wang S, Osgood AO, Chatterjee A. Uncovering post-translational modification-associated protein-protein interactions. Curr Opin Struct Biol 2022;74:102352.
36. Zamaraev AV, Kopeina GS, Prokhorova EA, Zhivotovsky B, Lavrik IN. Post-translational modification of caspases: the other side of apoptosis regulation. Trends Cell Biol 2017;27:322-339.
37. Wang WH, Yuan T, Qian MJ, Yan FJ, Yang L, He QJ, et al. Post-translational modification of KRAS: potential targets for cancer therapy. Acta Pharmacol Sin 2021;42:1201-1211.
38. Gong H, Zhong H, Cheng L, Li LP, Zhang DK. Post-translational protein lactylation modification in health and diseases: a double-edged sword. J Transl Med 2024;22:41.